Robustness Analysis of Sparsity Based Tumor Localization under Tissue Configuration Uncertainty

Mohammad Pourhomayoun, *Student Member, IEEE*, Mark Fowler, *Senior Member, IEEE and* Zhanpeng Jin, *Member, IEEE*

***Abstract*— Knowing the exact position of the tumor is a very critical prerequisite in radiation therapy. Since the position of the tumor changes because of respiration or patient movements, a real-time tumor tracking method must be applied during the process of radiation therapy in order to deliver a sufficient dose of radiation to the tumor region without damaging the surrounding healthy tissues.**

In this paper, we develop a novel tumor positioning method based on spatial sparsity and then we investigate the sensitivity of this method to the uncertainty of tissue configuration. The proposed method is easier to implement, non-iterative, faster and more accurate compared to common magnetic transponder based approaches. The performance of the proposed method is evaluated in two different cases: (1) when the tissue configuration is perfectly determined (acquired beforehand by MRI or CT) and (2) when there are some uncertainties about the tissue boundaries. The results demonstrate the satisfactory accuracy and high performance of the proposed method, even when the tissue boundaries are imperfectly known.

I. INTRODUCTION

Radiation therapy (also called Radiotherapy) is an effective method to combat cancerous tumors by delivering high doses of radiation to a tumor to kill or control the growth of malignant cells by damaging its DNA [1]. Three-dimensional conformal radiation therapy (3DCRT) and Intensity-Modulated Radiation Therapy (IMRT) have significantly enhanced the ability to deliver an accurate radiation dose to the target volumes. In these methods, the radiation is split into hundreds of thin beamlets targeting the tumor from various angles to achieve a better focus on the cancerous region and reduce the damage to the surrounding healthy cells [2]. In IMRT, beamlets can also have various radiation intensities and it helps to produce a treatment area that better conforms to the contour of the tumor [3]. IMRT is an effective and efficient tool to treat the concave-shape tumors such as tumors wrapping around the organs.

Knowing the exact position of the tumor is a very critical prerequisite in radiation therapy, because any slight bias in the position of the tumor will cause the radiation to be delivered to the surrounding healthy tissues rather than the tumor area, which not only degrades the performance of the treatment due to a lack of sufficient dose for the tumor treatment, but also it may cause severe side effects such as secondary cancer [2],[4]. However, the position of the tumor changes during radiation therapy because of respiration, gastro-intestinal, bladder filling, cardiac system or patient movements. Thus a *real-time* tumor tracking mechanism is highly desired in radiation therapy treatments in order to deliver a precise amount of radiation to the tumor region without damaging the surrounding healthy tissues [2],[4].

Various methods have been proposed in the literature for tumor tracking in IMRT treatments based on implanting several wired or wireless devices (called beacon) inside or in vicinity of the tumor [2]-[12]. The Calypso Localization system is one of the most prevalent methods that has been widely used for tumor positioning in prostate radiation therapy [7],[4]. In the Calypso system, three magnetic transponders are implanted in or near the target. Localization of the transponders is achieved using an electromagnetic array consisting of four electromagnetic coils to excite the transponders and 32 receiving coils picking up the response signal coming from the transponders. The positions of implanted transponders are calculated relative to the magnetic array based on the response measurements [7],[4]. There are several other electromagnetic tracking systems such as the methods proposed in [2], [12] that use the similar idea to track the tumor positions during the radiation therapy.

In [13], we presented preliminary results for a novel positioning and tracking method based on spatial sparsity in a 3D space with the goal of achieving better positioning accuracy. In the proposed method, we use only one wireless implantable RF transmitter (that has the potential to be smaller than magnetic transponders because there is no need for RLC resonance circuit) implanted inside or in the vicinity of the tumor. The implant plays the role of an emitter by transmitting an RF signal, which will be received by a sensor array mounted in a known position beneath or above the patient's body. Then, the received signals will be processed to estimate the position of the emitter (i.e., the implant), based on both time-of-arrival (TOA) and received signal strength (RSS) exploiting the spatial sparsity of the emitter in the 3D space. The performance of the proposed method was examined using Monte-Carlo computer simulation and the results demonstrate the high localization accuracy of our method (i.e., less than 2 mm error) and its robustness to multipath conditions caused by massive signal reflections at the boundaries of body organs [13].

It is manifest that in emitter localization problems, the number of emitters (even when we have more than one emitter) is usually much smaller than the number of all grid points in a fine grid on the x-y plane in a two-dimensional case, or x-y-z space in a three-dimensional scenario. Thus, by assigning a positive number to each one of the grid points containing an emitter and assigning zeros to the rest of the grid points, we will have a very sparse grid matrix that can

be reformed as a *sparse vector*. In this context, a *sparse vector* is a vector containing only a small number of non-zero elements [14]. Since each element of this grid vector corresponds to one grid point in the x-y-z space, we can estimate the location of the emitters by extracting the positions of all non-zero elements within the sparsest vector that can satisfy the delay relationship between transmitted signals and received signals [13], [15].

The human body is made up of various organs that consist of different types of tissues; thus, the electrical characteristics of the body – such as conductivity, power absorption, path loss, and relative permittivity – show significant heterogeneity and anisotropy. For example, the relative permittivity value varies for different tissues. Since the signal propagation velocity is expressed as a function of the relative permittivity, the propagation velocity and consequently the time-of-arrival (TOA) highly depends on the specific tissue layers that the signal passes through from the implant to the sensor. The power absorption parameters and path loss exponent also vary by thickness of the tissue [16].

We seek to estimate the average signal propagation velocity for the paths from each one of the grid points to the sensors. This estimation is accomplished after calculating the percentage of each tissue layer on the entire path that the signal travels through. Note that this velocity estimation can be performed in an off-line manner given the configuration of the body tissue layers, which could be acquired beforehand from MRI or CT systems [17]. Such propagation velocity information will be used later in the *real-time* localization and tracking step.

In [13] we assumed that the accurate configuration of human body tissues is available. Moreover, for the purpose of simplification, we used a uniform homogenous tissue configuration in the experimental simulation. However, given the fact that the localization performance in the proposed method highly relies on an accurate understanding of the tissue configuration, it is imperative to investigate the sensitivity of our method to the uncertainty of determined tissue layer boundaries. In this paper, we intend to address this problem by assessing the performance of our proposed sparsity-based approach in the case when the tissue configuration is not perfectly determined because of errors in estimating tissue boundaries. Unlike [13], in the simulation process of this study, the body model includes various tissues with different electrical characteristics (such as relative permittivity) and the RF signal is designed to pass through at least 3 different tissues (fat, muscle, lung tissue) to reach the receiver sensors.

II. Problem Formulation

Suppose that an implanted beacon transmits a signal and L sensors receive that signal. The complex baseband signal observed by the l^{th} sensor is

$$r_l(t) = \alpha_l s(t-\tau_l) + n_l(t) \qquad (1)$$

where $s(t)$ is the transmitted signal, τ_l is the signal delay, α_l is the path attenuation, and $n_l(t)$ is the noise.

In (1), α_l represents the path loss in addition to a constant phase shift. The path loss model in dB is given by [16],

$$PL(d) = PL(d_0) + 10\beta \log_{10}(d/d_0) + S, \quad d \geq d_0 \qquad (2)$$

where $PL(d)$ is the path loss at distance d, $PL(d_0)$ is the path loss at the reference distance d_0, β is the path loss exponent value and S is a zero mean Gaussian random variable (in dB) representing the shadowing effect, $S \sim N(0, \sigma_s^2)$ [16]. Table I shows the path loss [16].

TABLE I. PATH LOSS PARAMETERS: IMPLANT TO BODY SURFACE MODEL

Implant to Body Surface	PL(d_0) (dB)	B	σ_s (dB)
Deep Tissue	47.14	4.26	7.85
Near Surface	49.81	4.22	6.81

In free space, we can reasonably assume that the signal propagation velocity is constant. However, for the localization inside the human body the propagation velocity is not constant. We can calculate the average relative permittivity and average velocity for the path along which the signal is traveling as follows [17],

$$v_{avg} = \frac{c}{\sqrt{\varepsilon_{avg}}}$$
$$\varepsilon_{avg} = \sum_{i=1}^{N_I} \varepsilon_i p_i, \qquad (3)$$

where v_{avg} is the average propagation velocity, N_I is the number of different tissue layers on the path, ε_i is the relative permittivity of i^{th} tissue at desired frequency and p_i is the percentage of each tissue on the path. Table II shows the average relative permittivity of some of the body tissues [17]. We are able to obtain the v_{avg} for each path using (3), given the configuration of body tissues that was acquired beforehand from MRI or CT systems [13], [17].

TABLE II. THE AVERAGE RELATIVE PERMIITTIVITY OF BODY TISSUES

Tissue	Muscle	Fat	Bone	Lung	Stomach	Intestine	Tendon
ε_r	47.83	4.08	7.85	42.56	56.99	50.67	37.61

Assume that each sensor collects N_s signal samples at sampling frequency $F_s = 1/T_s$. Then we have

$$\boldsymbol{r}_l = \alpha_l \boldsymbol{D}_l \boldsymbol{s} + \boldsymbol{n}_l \qquad (4)$$
$$\boldsymbol{s} = [s(t_1),\ s(t_2),\ \ldots\ ,\ s(t_{Ns})]^T$$
$$\boldsymbol{r}_l = [r_l(t_1),\ r_l(t_2),\ \ldots\ ,\ r_l(t_{Ns})]^T$$
$$\boldsymbol{w}_l = [w_l(t_1),\ w_l(t_2),\ \ldots\ ,\ w_l(t_{Ns})]^T$$

where $\boldsymbol{r}_l = [r_l(t_1),\ r_l(t_2),\ \ldots,\ r_l(t_{Ns})]^T$ is the vector containing N_s samples of the received signal by l^{th} sensor, $\boldsymbol{s} = [s(t_1),\ s(t_2),\ \ldots,\ s(t_{Ns})]^T$ is N_s samples of the transmitted signal, $\boldsymbol{n}_l$ is the noise vector and $\boldsymbol{D}_l$ is the time sample shift operator by $k_l = (\tau_l / T_s)$ samples where $\tau_l = (d_l / v_{avg,l})$ is delay, d_l is the distance between emitter and the l^{th} sensor and $v_{avg,l}$ is the average velocity on the path from emitter to the l^{th} sensor derived from (3). We can write $\boldsymbol{D}_l = \boldsymbol{D}^{k_l}$ where $\boldsymbol{D}$ is an $N_s \times N_s$ permutation matrix defined as $[\boldsymbol{D}]_{ij} = 1$ if $i = j+1$, $[\boldsymbol{D}]_{0,N-1} = 1$ and $[\boldsymbol{D}]_{ij} = 0$ otherwise.

In this study, we estimate the target location in the two-dimensional (*x*-*y*) plane. However, it can be easily extended into a three-dimensional case.

Now, we assign a number $z_{x,y}$ to each one of the grid points (*x*,*y*). Assume that $z_{x,y} = 1$ for the grid point containing the implant beacon and $z_{x,y} = 0$ for the rest of the grid points. Thus, the signal vector received by l^{th} sensor will be

$$\boldsymbol{r}_l = \sum_x \sum_y z_{x,y} \alpha_{l,x,y} \boldsymbol{D}_{l,x,y} \boldsymbol{s} + \boldsymbol{n}_l \ , \qquad (5)$$

where $\boldsymbol{D}_{l,x,y}$ is the time sample shift operator w.r.t sensor *l* assuming that the emitter is located in the grid point (*x*,*y*) and the summations are over all grid points in the desired (*x*,*y*) range. Note that $\boldsymbol{D}_{l,x,y}$ and $\alpha_{l,x,y}$ are known in (5) since the location of the sensor *l* and each grid point (*x*,*y*) is known and we are able to find the path loss and delay from (2) and (3) for the distance from grid point (*x*,*y*) to the sensor *l*. The unknown term is $z_{x,y}$ which represents the grid point containing the implant beacon. Now, if we reform all of the grid points in a column vector and re-arrange the indices, we will have

$$\boldsymbol{r}_l = \sum_{n=1}^{N} z_n \alpha_{l,n} \boldsymbol{D}_{l,n} \boldsymbol{s} + \boldsymbol{n}_l . \qquad (6)$$

Now, we define the matrix $\boldsymbol{\Gamma}_n$ as the delay and path-loss operator with respect to all *L* sensors, assuming that the received signal comes from the grid point *n*:

$$\boldsymbol{\Gamma}_n = \left[\alpha_{1,n} \boldsymbol{D}_{1,n} \quad \alpha_{2,n} \boldsymbol{D}_{2,n} \quad \cdots \quad \alpha_{L,n} \boldsymbol{D}_{L,n} \right]_{N_s \times LN_s} \qquad (7)$$

Then, we can define $\boldsymbol{\theta}_n, n \in \{1, 2, \ldots, N\}$ as an $LN_s \times 1$ vector containing all signals received by all *L* sensors when the emitter is in grid point *n* as,

$$\boldsymbol{\theta}_n = \boldsymbol{\Gamma}_n^{\ T} \times \boldsymbol{s}_n \qquad (8)$$

where $(.)^T$ is the matrix transpose.

Now, if we arrange all vectors $\boldsymbol{\theta}_n$ for *n*:1...*N* as the columns of a matrix $\boldsymbol{\Theta}$ as,

$$\boldsymbol{\Theta} = [\boldsymbol{\theta}_1 \quad \boldsymbol{\theta}_2 \quad \ldots \quad \boldsymbol{\theta}_N]_{LN_s \times N} \ , \qquad (9)$$

then we have

$$\boldsymbol{r} = \boldsymbol{\Theta} \times \boldsymbol{z} + \boldsymbol{n} \qquad (10)$$

where $\boldsymbol{r} \triangleq [\boldsymbol{r}_1^T \quad \boldsymbol{r}_2^T \quad \ldots \quad \boldsymbol{r}_L^T]^T_{LN_s \times 1}$ is the vector of all *L* received signals, $\boldsymbol{z} = [z_1 \quad z_2 \quad \ldots \quad z_N]^T_{N \times 1}$ is the sparse vector of *z*-values assigned to each grid point and $\boldsymbol{n}$ is the noise.

Now, we can estimate the location of the emitter by extracting the position of non-zero elements of the sparsest vector that satisfies the delay and path-loss relationship between transmitted signals and received signals. In other words, because the signals are noisy, we need to find a sparse vector that minimizes the cost which is defined as the Euclidean distance between $\boldsymbol{r}$ and $\boldsymbol{\Theta} \times \boldsymbol{z}$ in equation (10). In principle, sparsity of the grid vector can be enforced by minimizing its ℓ_0-norm which is defined as the number of non-zero elements in the vector. However, since the ℓ_0-norm minimization is an NP-hard non-convex optimization problem, it is very common to approximate it with ℓ_1-norm minimization, which is a convex optimization problem and also achieves the sparse solution very well [14].

Thus, we can solve our problem by forming the regularized *BPDN* (*Basis Pursuit Denoising*) *problem* as [18]:

$$\hat{\boldsymbol{z}} = \arg\min\left(\left\| \boldsymbol{\Theta} \times \boldsymbol{z} - \boldsymbol{r} \right\|_2 + \lambda \left\| \boldsymbol{z} \right\|_1 \right) \qquad (11)$$

where $\| . \|_p$ is the ℓ_p-norm defined as $\| v \|_p = \sqrt[p]{\sum_i |v_i|^p}$.

III. Simulation Results and Conclusion

We examined the performance of the proposed method using Monte-Carlo computer simulation with 100 runs each time for two different cases: (1) when the body tissue configuration is perfectly known and (2) when there is some uncertainty on the tissue configuration and tissue boundaries. Figure 1 shows an example when the signal (emitted by the target implant) travels through three different tissues including organ tissue (such as lung tissue), muscle and fat to reach the external sensors. In this case the sensors are mounted on the body surface, although they can also be mounted anywhere above or beneath the patient's body. Figure 1-(a) shows the case when the tissue configuration is perfectly known and Figure 1-(b) demonstrates the case when the tissue boundaries are known with uncertainty. To simulate this uncertainty, we added *unknown* random noise to the simulated perfect tissue boundaries.

Figure 2 shows the simulation results for the two cases illustrated in Figure 1. Figure 2-(a) shows a simple pattern for tumor (or implant) movement in the X direction. Figure

2-(b) shows the RMS (Root Mean Square) Errors of the implant localization results for the aforementioned two scenarios. In this simulation, we chose the parameters such as SNR=10dB, the signal is BPSK modulated with carrier frequency 405 MHz and the sampling frequency is 100 MHz. We use a sensor array of only 8 sensors to receive the RF signal from the implanted emitter. In these simulations, we also simulated the massive multipath condition (signal reflections from tissue boundaries) using reflector points at randomly chosen locations. The standard deviation of the unknown noise added to the boundary surfaces was 3mm (Std = 3mm).

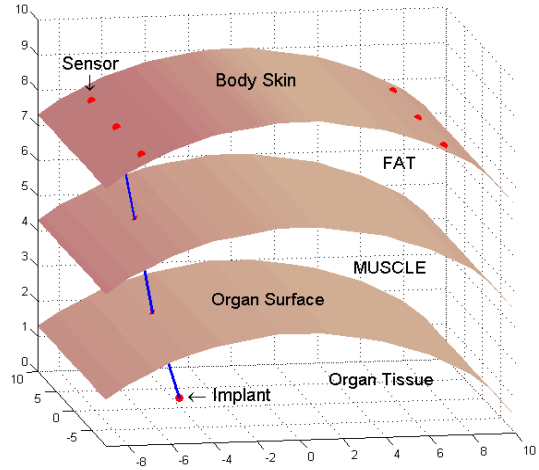

(a)

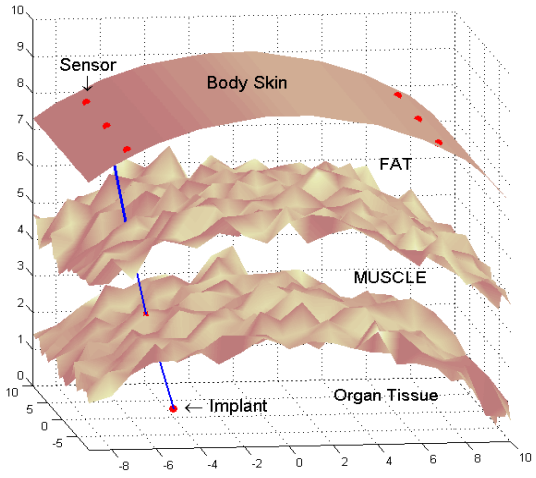

(b)

Figure (1): A sample tissue configuration. The top surface is the body skin, the middle surface is the boundary between fat and muscle and the third surface is the organ surface (such as lung surface) which is the boundary between muscle and organ tissue. The red points on the body skin are the sensors and the blue line is the line-of-sight from one of the sensors to the emitter. (a) perfectly known boundaries (b) approximately known boundaries generated by adding unknown noise to the boundary surfaces.

The simulation results show the accurate localization and high performance of this method. The localization error is less than 2mm when the tissue configuration is perfectly known and less than 2.7mm (in the worst case) for underdetermined tissue boundaries. It is significant that a boundary error level of 3mm only increased the localization error by 0.7mm. It is worth mentioning that in these simulations we used only 16 signal samples for the purpose of reducing the computational load. The localization performance and accuracy can be further improved by increasing the number of samples.

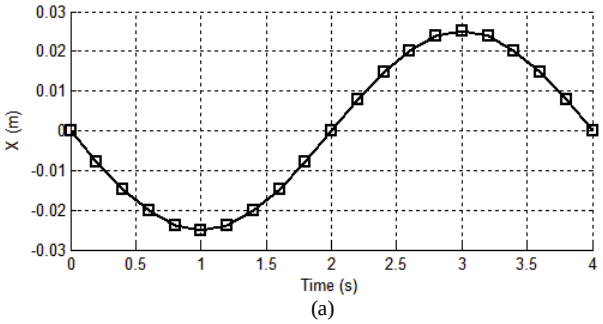

(a)

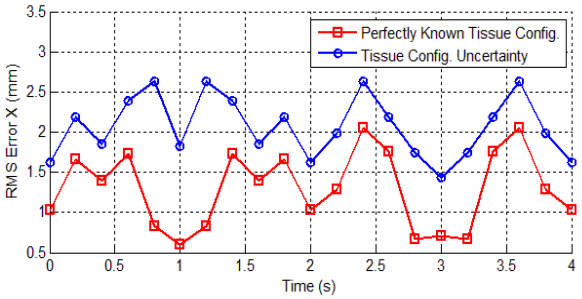

(b)

Figure (2): (a) A simple pattern for tumor (or implant) movement in X direction, (b) RMS Error for implant location estimation for the movement pattern in (a) in two cases: when the tissue boundary surfaces are perfectly known (red curve) and when there is some uncertainty about the boundary surfaces (blue curve).

In another simulation, we ran Monte-Carlo algorithms for various numbers of sensors (4, 8, 12 and 16 sensors with 100 runs each time), under the multipath and shadowing conditions for the two cases. In this simulation, the position of the implant was randomly chosen. Figure 3 shows the RMS errors versus the number of sensors for estimating the location of the target in a 2D (x,y) plane. Not surprisingly, the accuracy is better when we know the exact configuration of the body tissues. However, even considering a more practical case that the exact tissue configuration information is not available and there is certain level of uncertainty in the determined tissue boundaries, we can still achieve very accurate location estimation (less than 2 mm error in the worst case). We can also see that in both cases, the accuracy gets better by increasing the number of sensors.

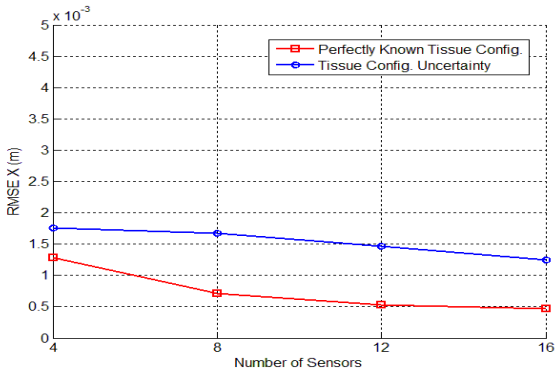

(a)

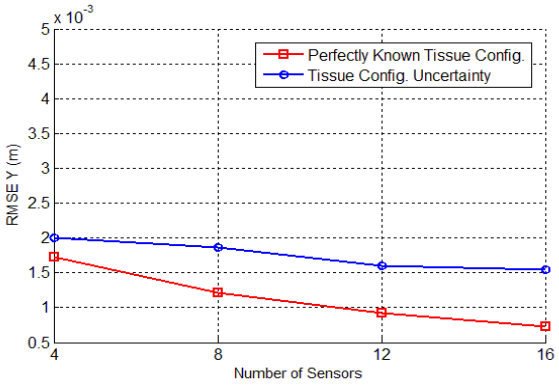

(b)

Figure (3): RMS Error for X and Y versus Number of sensors for the two cases.

REFERENCES

[1] C. M. Washington and D. T. Leaver, *Principles and Practice of Radiation Therapy*, 2nd ed. St. Louis, MO: Mosby, 2003.

[2] Wing-Fai Loke, Tae-Young Choi, Maleki, T., Papiez, L., Ziaie, B., Byunghoo Jung, "Magnetic Tracking System for Radiation Therapy," IEEE Trans. on Biomedical Circuits and Systems, Vol. 4, No. 4, 2010.

[3] D. I. Lewin, "Intensity-modulated radiation therapy," *Computer Science Eng.*, vol. 4, no. 5, pp. 8–9, Sep./Oct. 2002.

[4] Andreas W. Rau, et al., "Real-time tumor localization with electromagnetic transponders for image-guided radiotherapy applications," *PhD Dissertation*, 2009.

[5] S. Dieterich and Y. Suh, *Treating Tumors That Move With Respiration*. New York: Springer, 2007, pp. 3–13.

[6] A. P. Shah, et al., "Expanding the Use of Real-Time Electromagnetic Tracking in Radiation Oncology," Journal of Applied clinical Medical Physics, Vol. 12, No. 4, 2011.

[7] P. Kupelian, et al. Clinical experience with the Calypso 4D localization system in prostate cancer patients: implantation, tolerance, migration, localization and real time tracking. Int J Radiat Oncol Biol Phys. 2005;63(Suppl 1):S197.

[8] W. Loke, et al., "A 0.5-V Sub-mW Wireless Magnetic Tracking Transponder for Radiation Therapy," VLSI Circuits (VLSIC) Symposium, 2011.

[9] Tae-young Choi, et al., "Wireless Magnetic Tracking System for Radiation Therapy," Life Science Systems and Applications Workshop, 2009.

[10] Kindblom J, et al. High precision transponder localization using a novel electromagnetic positioning system in patients with localized prostate cancer. Radiother Oncol. 2009.

[11] A. Plotkin and E. Paperno, "3-D magnetic tracking of a single subminiature coil with a large 2-D array of uniaxial transmitters," *IEEE Trans. Magn.*, vol. 39, no. 5, pp. 3295–3297, Sep. 2003.

[12] E. Paperno and P. Keisar, "Three-dimensional magnetic tracking of biaxial sensors," *IEEE Trans. Magn.*, vol. 40, no. 3, May 2004.

[13] M. Pourhomayoun, M. L. Fowler and Zhanpeng Jin, "A Novel Method for Tumor Localization and Tracking in Radiation Therapy," *Asilomar Conference on Signals, Systems and Computers*, 2012.

[14] R. G. Baraniuk. "Compressive Sensing". *IEEE Signal Processing Magazine*, 118–120, July 2007.

[15] M. Pourhomayoun and M. Fowler**, "**Spatial Sparsity Based Emitter Localization," *Conf. on Information Sciences and Sys., CISS*, 2012.

[16] K. Sayrafian-Pour, et al., "A statistical path loss model for medical implant communication channels," in *Personal, Indoor and Mobile Radio Communications,IEEE 20th International Symposium on*, 2009.

[17] M. Kawasaki , R. Kohno, "A TOA Based Positioning Technique of Medical Implanted Devices," *international Symposium on Medical information & communication technology*, 2009.

[18] M. F. Duarte, Y. C. Eldar, "Structured Compressed Sensing: From Theory to Applications", *IEEE Transactions on Signal Process.*, 2011.